Fingerprint Liveness Detection based on Histograms of Invariant Gradients

Carsten Gottschlich
Institute for Mathematical Stochastics
University of Göttingen
gottschlich@math.uni-goettingen.de

Emanuela Marasco
Lane Department CSEE
West Virginia University
emanuela.marasco@mail.wvu.edu

Allen Y. Yang
EECS Department
UC Berkeley
yang@eecs.berkeley.edu

Bojan Cukic
Department of Computer Science
University of North Carolina at Charlotte
bcukic@uncc.edu

Abstract

Security of fingerprint authentication systems remains threatened by the presentation of spoof artifacts. Most current mitigation approaches rely upon the fingerprint liveness detection as the main anti-spoofing mechanisms. However, liveness detection algorithms are not robust to sensor variations. In other words, typical liveness detection algorithms need to be retrained and adapted to each and every sensor used for fingerprint capture. In this paper, inspired by popular invariant feature descriptors such as histograms of oriented gradients (HOG) and the scale invariant feature transform (SIFT), we propose a new invariant descriptor of fingerprint ridge texture called histograms of invariant gradients (HIG). The proposed descriptor is designed to preserve robustness to variations in gradient positions. Spoofed fingerprints are detected using multiple histograms of invariant gradients computed from spatial neighborhoods within the fingerprint. Results show that proposed method achieves an average accuracy comparable to the best algorithms of the Fingerprint Liveness Detection Competition 2013, while being applicable with no change to multiple acquisition sensors.

1. Introduction

The deployment of fingerprint recognition systems is growing. The ease of use and low error rates are the main factors that contribute to their widespread use [17]. Subsequently, the interest in guaranteeing the reliability of these systems has increased as well. Several issues pertaining to the security of fingerprint systems under spoof artifact presentations have arisen. Fingerprint ridges can be modeled using artificial materials such as latex, silicone, or gelatin and maliciously employed to gain unauthorized access to the system protected by the fingerprint sensor [28] [26] [15]. The risk of spoof attacks is becoming serious and it involves realistic cases. In March 2013, spoof fingerprints were maliciously used by a doctor to forge the check-in of absent coworkers[1]. In September, only two days after the iPhone5S was released, its vulnerability to spoof fingerprints was announced[2].

This problem has been handled through the development of various anti-spoofing mechanisms most of which focused on liveness detection approaches [28]. Liveness detection refers to the ability of a system to discriminate between human live fingerprints and spoof artifacts [26]. Error rates of liveness detection approaches reported in the literature are generally not low enough to satisfy requirements for high security, as reported by Liveness Detection Competitions [23] [31] [8]. Existing algorithms are limited by their learning-based nature which implies dependence on both the sensor used for acquiring data and the specific set of materials used for representing the spoof class when training [21]. To the best of our knowledge, the scientific literature lacks anti-spoofing techniques robust to variations induced in the images by the sensor. In particular, minutiae locations are affected by variations induced by the acquisition device and, due to this, may imply changes in liveness detection accuracy across different optical sensors [19]. Although approaches such as histograms of oriented gradients (HOG) and the scale invariant feature transform (SIFT) are efficient and popular in computer vision, they have note been used for implementing anti-spoofing techniques.

In this paper, inspired by the invariant feature descriptors HOG and SIFT, we propose a new invariant descriptor of fingerprint ridge texture called histograms of invariant

[1] http://nexidbiometrics.com/brazilian-doctor-arrested-for-using-fake-fingerprints/

[2] http://secureidnews.com/news-item/apples-touch-id-spoofed/

gradients (HIG). In the proposed approach, liveness is predicted based on local histograms which count occurrences of gradient orientation and magnitude in a local region of the fingerprint image. Local gradients are estimated by preserving independence of the precise gradient positions. HIG features this innovative aspect which is promising for dealing with changes in liveness detection accuracy across different capture devices.

This paper is organized as follows. In Section 2, we describe the state-of-the-art in the fingerprint anti-spoofing strategies. Section 3 presents the proposed approach. Section 4 discusses the evaluation procedure and experimental results. Section 5 draws conclusions and future research directions.

2. Related Works

Liveness detection currently represents the countermeasure most commonly used for minimizing the risk associated with spoof presentations. The detection can be categorized as being hardware- or software-based [29] [20]. Hardware-based solutions usually exploit characteristics of vitality such as temperature of the finger, electrical conductivity of the skin, pulse oximetry [27]. These approaches require the integration of additional hardware into the biometric sensor which makes the device more expensive; additionally, an improper integration can result in a vulnerable scenario where a spoof artifact is placed on the fingerprint sensor while any live finger is placed on the added hardware. Software-based liveness detection represents a cheaper and *non-invasive* solution. Methods in this category can exploit characteristics derived from multiple frames of the same fingerprint, referred to as *dynamic*, or from a single impression, referred to as *static*. Static approaches appear more suitable for achieving high performance, in terms of time and accuracy, required in operational scenarios.

A physiological phenomenon of live human fingers which has been investigated in past studies is perspiration. The corresponding spatial moisture pattern can be quantified by temporal gray-level changes between two sequential images. Abhyankar and Schuckers [1] isolated the perspiration pattern through changes in wavelet coefficients between two images. In particular, high frequency components due to the circular transitions from dark to white around pores are captured with wavelet packets, while low frequency components due to the occurrence of pores are captured via multi-resolution analysis (MRA). The corresponding liveness measure is computed as the total energy associated to the considered frequency bands. Reported equal error rate (EER) is of 13.85%. Perspiration has been be exploited statically as well by processing only one image [30]. Based on the observation that pixels of spoofs are mainly distributed in the dark gray levels ($<$150), Tan and Schuckers derived two features: *i) Gray Level 1 ratio*, computed as the ratio between the number of pixels with gray level (150, 253) and the number of pixels with gray-level ranging in (1, 149); *ii) Gray Level 2 ratio*, computed as the ratio between the number of pixels with gray level (246, 256) and the number of pixels with gray-level ranging in (1, 245).

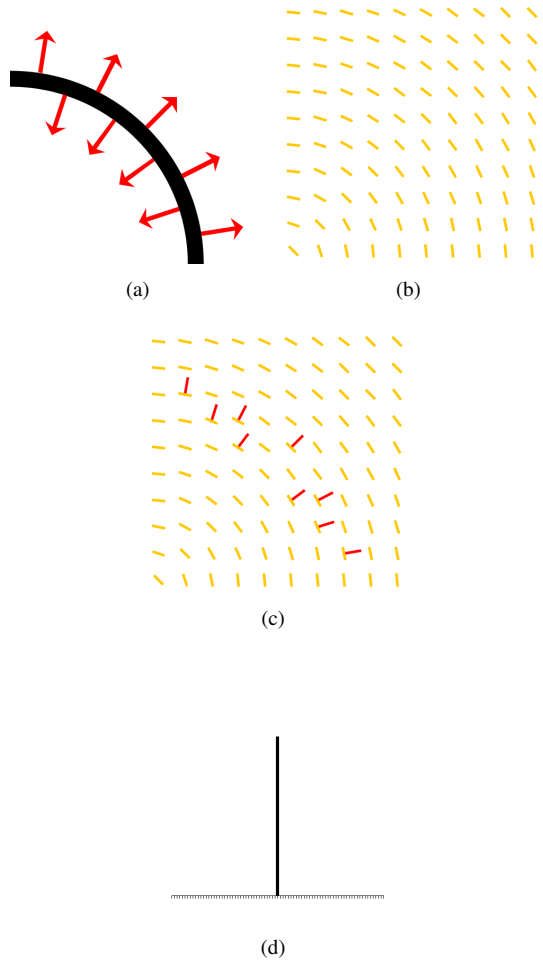

Figure 1. The basic steps for computing the histogram of invariant gradients are: (a) computing the image gradients (red arrows on the black ridge line) and (b) estimating the orientation field. Then, the angle between unsigned gradients and the local orientation at each pixel (c) determines in which orientation bin the gradient is sorted. Finally, the histogram of invariant gradients (d) is a summary statistic of all gradient lengths in a local neighborhood. In this noise-free synthetic example, all gradients are perpendicular to the local orientation and their invariant representation is sorted into the bin centered at 90° (d).

Several studies analyze variations in texture (e.g., morphology, smoothness) exhibited by spoof and live fingerprints. Moon *et al.* [24] modeled the fingerprint surface by using the standard deviation of the residual noise which represents an indicator of texture coarseness. This allows

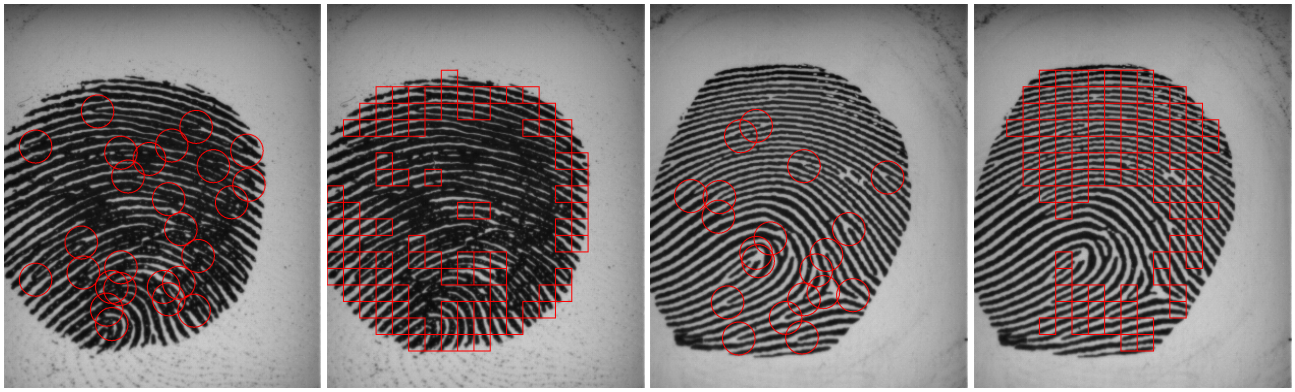

(a) (b) (c) (d)

Figure 2. Two fingerprints from the LivDet 2013 Biometrika database: a print of a real finger on the left (a/b) and an image acquired from a spoof made of Eco Flex on the right (c/d). Two ways of geometric partitioning are considered for computing the descriptor: for the *minutiae circle* approach, gradients within a circle of radius 16 pixels around minutiae locations are taken into account for computing the histogram in (a) and (c). For the *dense block packing* approach, the image is divided into blocks of 16×16 pixels and the 100 blocks with the highest sum of gradient vector lengths are chosen as depicted in (b) and (d).

for distinguishing between live and spoof fingerprints since the surface texture of a live finger is generally less coarse than a spoof. Furthermore, since fingerprints exhibit oriented texture-like pattern, Nikam *et al.* [25] extracted Gabor filter-based features to capture local frequency and orientation information. The gray level distribution of single pixels is modeled by the first order statistics, while the joint gray level function between pairs of pixels is modeled by the second order statistics. Marasco and Sansone successfully investigated the joint contribution of the most robust texture and perspiration-based measures [22]. A novel set of features for detecting liveness based on the Local Phase Quantization of the fingerprint image has been defined by Ghiani *et al.* [7]. Recently, Gragnaniello *et al.* [13] proposed a method based on the Weber's law while Ghiani *et al.* [6] evaluated binarized statistical image features in which the fingerprint representation is obtained by learning filters, instead of manually tuning them. Quality measures such as *strength* and *clarity* of fingerprint ridges have been exploited for anti-spoofing purposes too. In particular, the ridge continuity is captured by measuring the continuity of the orientation fields [5]. Espinoza *et al.* [4] proposed a method based on comparing pore quantity between spoof and live fingerprint images.

3. Histograms of Invariant Gradients (HIG)

3.1. Basic Algorithm

In this section, we describe the proposed approach which is based on an approximation of image gradients invariant not only to rotation and translation but also to curvature and deformation. This effort aims to design an algorithm robust device and spoof material diversity. Liveness can be predicted based on multiple histograms of these invariant gradients computed in local neighborhoods. The image gradient operator estimates the maximum rate of the gray levels increase per unit distance. For an image I, the gradient of I at coordinates (x, y) is defined as the following vector:

$$\nabla \mathbf{I} = \begin{bmatrix} G_x \\ G_y \end{bmatrix}, \tag{1}$$

$$mag(\nabla \mathbf{I}) = [G_x^2 + G_y^2]^{1/2}. \tag{2}$$

G_x corresponds to $\frac{\partial I}{\partial x}$, the differences in x (horizontal) direction, G_y corresponds to $\frac{\partial I}{\partial y}$, the differences in y (vertical) direction [9], and $mag(\nabla \mathbf{I})$ is the gradient magnitude or length.

Image Gradients Estimation. Image gradients are computed for each pixel using the Sobel filter, see Figure 1 (a). To achieve conditions of invariance described above, in our approach local gradients are compensated by normalizing relative gradients with respect to the global orientation field. The orientation field is estimated by the line sensor method [11], see Figure 1 (b). The *local orientation* is defined as the tangent to the fingerprint ridge. This normalization results in an *invariant representation* of each gradient (see Figure 1 (c)).

Histograms of Invariant Gradients. Histograms of *invariant gradients* (see Figure 1 (d)) are computed in local neighborhoods by considering the following two geometric partitions (see Figure 2):

- *Minutiae Circles*. Minutiae are extracted and for each minutia i, a histogram of invariant gradients is com-

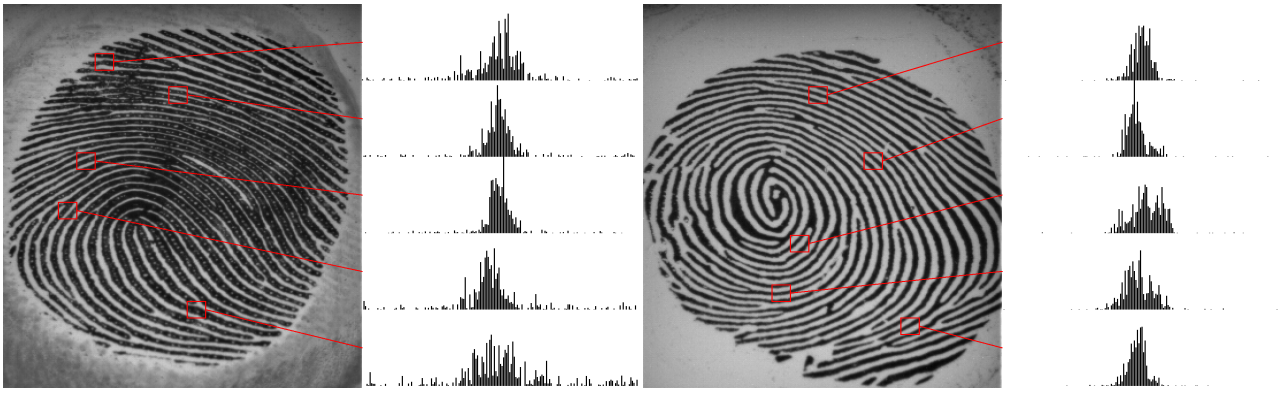

(a) (b)

Figure 3. Histograms with 180 orientation bins (the leftmost bin corresponds to 0°) are displayed for 5 out 100 blocks for an image of a real finger (left) and a spoof (right). High bars around the center of the histograms indicate that most gradients are orthogonal to the local orientation.

	SIFT	**HOG**	**HIG**
Gradient directions are normalized with respect to	keypoint direction	global, fixed coordinate system for the whole image	local orientation at each pixel
Histograms and bins per descriptor	4×4 histograms with 8 directional bins for each keypoint	1 histogram with 9 orientation bins for each cell and 4-9 cells per HOG	1 histogram with 180 orientation bins for each circle or block
Gradients signed (0-360°) or unsigned (0-180°)	signed	unsigned	unsigned
Invariance to rotation and translation	yes	no	yes
Invariance to curvature and deformation	no	no	yes
Typical number of descriptors per image	1000-2000 keypoints	4000 detection windows	around 20-40 minutiae circles or top 100 blocks

Table 1. Summary of similarities and differences regarding key properties of SIFT [16], HOG [3] and our approach.

puted taking into account all gradients within a circle of radius $r = 16$ pixel around the minutia location (x_i, y_i).

- *Dense Block Packing*. The whole image (the fingerprint foreground) is divided into non-overlapping blocks of size 16×16 pixels. For each block, we calculate the sum of gradient lengths inside that block. The first $t = 100$ blocks with biggest sum of gradient lengths are chosen.

Histograms are obtained after sorting each invariant gradient into the nearest of $n = 180$ orientation bins. Since the orientation resolution of the histogram is very fine, no weighted voting into neighbooring is performed. Each histogram is normalized by L2-normalization.

Let h be the unnormalized histogram of summed up gradient lengths per bin, $||h||_k$ its k-norm and ϵ be a very small constant. For L2-normalization we compute

$$h := h/\sqrt{||h||_2^2 + \epsilon}. \tag{3}$$

The normalized histograms are used as features for training by a support vector machine with a linear kernel ($C = 1.0$). Histograms obtained from spoof fingerprints are used as negative examples ($y = 0$) and histograms derived from images of live fingers are used as positive examples ($y = 1$). A model learned on the training data is applied to predict whether a histogram originated from a spoof ($y = 0$) or a real finger ($y = 1$). The average of all predictions for one image is considered as the *liveness score* s. Based on the average prediction score s and the determined threshold, an image is classified as spoof or live. The main steps of the proposed approach are summarized in Algorithm A.

Algorithm A. Histograms of Invariant Gradients.

Input:
Let $I(x, y)$ be the original Fingerprint Image.

Steps:
1. Compute Image Gradients from $I(x, y)$.
2. Estimate Orientation Field from $I(x, y)$.
3. Compute Geometric Partitioning.
Option 3.1.: Circles of radius 16 pixels around minutiae locations.
Option 3.2.: Top 100 blocks of 16×16 pixels with the biggest sum of gradient lengths.
4. Obtain Invariant Gradients by normalizing gradient directions with respect to the local orientation.
5. Compute Histogram of Invariant Gradients by
adding gradients lengths to the corresponding orientation bins.
6. Histogram Normalization by L2-normalization.

Output:
k Histograms of Invariant Gradients.

A comparison of the key properties of SIFT, HOG and the proposed invariant gradient representation is summarized in Table 1. Compared to SIFT and HOG, HIG relies on much less number of feature points to describe the appearance of fingerprint ridge texture, which makes it computationally efficient. At the same time, it inherits the robustness of SIFT and HOG that can effectively compensate the variations in typical fingerprint images in terms of illumination and orientation. Such capabilities enable a liveness detection algorithm to achieve good accuracy in cross-device scenarios.

3.2. Variations

In addition, we propose an extension of the descriptor in which, additional to the 180 orientation bins, two more features are considered: the gradient coherence in a block as defined in Equation 10 of [12] and the difference between the largest and smallest gradient length in a block. This descriptor with 182 features is referred to as "HIG dense block packing extended" in Table 2, and "HIG dense block packing combined" chooses the best of these two variants in the training set. Using the available training images, we investigated conceivable alternatives to the parameters and choices previously described:

- Different radii around minutiae locations.
- A geometry with a central circular cell and four cells on an annulus with an expanded radius as in the C-HOG of [3].
- Different block sizes and blocks consisting of two or more cells to allow overlap.
- Different number of blocks per image.
- Different number of orientation bins.
- Considering signed instead of unsigned gradients.
- Four histogram normalization schemes: L1, L1-sqrt, L2 and L2-Hys.
- Different kernels and parameters for the support vector machine.

We also explored histograms of gradients relative to the minutiae direction, similar to SIFT descriptor. However, using these histograms as features decreased the accuracy considerably in comparison to the proposed invariant gradient representation.

4. Experimental Results

4.1. Benchmark Data Set

The LivDet2013 [8] data set consists of fingerprint images acquired with four different sensors:

- Biometrika FX2000 (optical sensor with 569 DPI resolution and 312×372 pixels image size).
- Italdata ET10 (optical sensor with 500 DPI resolution and 640×480 pixels image size).
- Crossmatch L Scan Guardian (optical scanner with 500 DPI resolution and 800×750 pixels image size).
- Swipe sensor with 96 DPI resolution and 208×1500 pixels image size.

According to the description in [8], there are training and test sets comprising 1,000 images for each of the four sensors and for each of the two scenarios 'live' and 'spoof', with the exception of the CrossMatch device and the swipe sensor in the scenario 'live' for which 1,250 training and 1,250 test images are available, summing up to a total of 17,000 images. The results in this paper are based on 16,853 images which were made available for download by the organizers of the competition.

4.2. Evaluation Procedure

Histograms are computed for all training images in each considered database. Using all training images we determine the threshold which maximizes the accuracy for that training set. During the test phase, histograms are computed for each image, as previously described. The learned SVM model is applied to predict a fake finger or a live finger. Experiments were performed using LIBSVM [2].
The liveness detection accuracy a is computed as follows:

$$a = \frac{C}{N}, \tag{4}$$

LivDet 2013	Biometrika	Italdata	Crossmatch	Swipe	Average
Anonym2	98.20	99.40	45.20	94.19	84.25
Dermalog	98.30	99.20	44.53	96.47	84.63
UniNap1	95.30	96.50	68.80	85.93	86.63
HIG minutiae circle	95.70	89.40	60.04	67.59	78.18
HIG dense block packing	96.10	91.70	65.87	85.56	84.81
HIG dense block packing extended	89.10	98.30	71.24	81.89	85.13
HIG dense block packing combined	**96.10**	**98.30**	**71.24**	**85.56**	**87.80**

Table 2. The rate of accuracy, in percents, for the four sensor databases of LivDet 2013 and the average accuracy. The results of the best three algorithms of LivDet 2013 in terms of average accuracy are cited from [8].

where C is the number of correct decisions (classifying an image of an alive finger as 'alive' and classifying an image of a fake finger as 'spoof') and N is the number of all decisions.

4.3. Results and Discussion

Table 2 reports the accuracy of the best algorithms from LivDet 2013 and the proposed method. These results show that proposed method achieves average accuracy similar to the best algorithms in LivDet 2013. A major advantage of the invariant gradient representation is that it creates very few additional computational costs.
Most fingerprint algorithms are based on minutiae for matching [17]. Typical processing steps before minutiae extraction are segmentation, orientation field (OF) estimation and image enhancement [10]. Therefore, computing the image gradients and estimating the OF can be regarded as 'free' assuming the liveness detection module is used in combination with algorithms which require these steps [18]. Other software-based liveness detection methods apply features like the wavelet-Markov local descriptor [14], which may not be utilized by the matching algorithm and therefore impose extra burden with regard to the computational costs.

5. Conclusions

Results show that proposed method achieves a comparable average accuracy with the best algorithms on LivDet 2013 using the same evaluation protocol; however, this evaluation procedure limits the evaluation of the algorithm with respect to the robustness to device diversity. We will extend experiments by testing with different materials to represent the spoof class and to demonstrate interoperability of the proposed liveness detector.

Acknowledgement

C. Gottschlich gratefully acknowledges the support of the Felix-Bernstein-Institute for Mathematical Statistics in the Biosciences and the Volkswagen Foundation. E. Marasco and B. Cukic acknowledge the support of the Center for Identification Technology Research (CITeR), West Virginia University. E. Marasco thanks Prof. Silvio Savarese, Computational Vision and Geometry Lab, Stanford University, for useful discussions about the Histograms of Oriented Gradients approach.

References

[1] A. Abhyankar and S. Schuckers. Integrating a wavelet based perspiration liveness check with fingerprint recognition. *Pattern Recognition*, 42(3):452–464, March 2009.

[2] C. Chang and C. Lin. LIBSVM: a library for support vector machines. *ACM Transactions on Intelligent Systems and Technology*, 2(3):1–27, April 2011.

[3] N. Dalal and B. Triggs. Histograms of oriented gradients for human detection. In *Proc. CVPR*, pages 886–893, San Diego, CA, USA, June 2005.

[4] M. Espinoza and C. Champod. Using the number of pores on fingerprint images to detect spoofing attacks. In *Proc. ICHB*, pages 1–5, Hong Kong, China, November 2011.

[5] J. Galbally, F. Alonso-Fernandez, J. Fiérrez, and J. Ortega-Garcia. A high performance fingerprint liveness detection method based on quality related features. *Future Generation Comp. Syst.*, pages 311–321, 2012.

[6] L. Ghiani, A. Hadid, G.L Marcialis, and F. Roli. Fingerprint liveness detection using binarized statistical image features. *Proc. BTAS*, pages 1–6, 2013.

[7] L. Ghiani, G.L. Marcialis, and F. Roli. Fingerprint liveness detection by local phase quantization. *Proc. ICPR*, pages 1–4, November 2012.

[8] L. Ghiani, D. Yambay, V. Mura, S. Tocco, G.L. Marcialis, F. Roli, and S. Schuckers. LivDet 2013 Fingerprint liveness detection competition 2013. In *Proc. ICB*, pages 1–6, Madrid, Spain, June 2013.

[9] R.C. Gonzalez and R.E. Woods. *Digital Image Processing*. Prentice Hall, Upper Saddle River, NJ, USA, 2002.

[10] C. Gottschlich. Curved-region-based ridge frequency estimation and curved Gabor filters for fingerprint image enhancement. *IEEE Transactions on Image Processing*, 21(4):2220–2227, April 2012.

[11] C. Gottschlich, P. Mihăilescu, and A. Munk. Robust orientation field estimation and extrapolation using semilocal line sensors. *IEEE Transactions on Information Forensics and Security*, 4(4):802–811, December 2009.

[12] C. Gottschlich and C.-B. Schönlieb. Oriented diffusion filtering for enhancing low-quality fingerprint images. *IET Biometrics*, 1(2):105–113, June 2012.

[13] D. Gragnaniello, G. Poggi, C. Sansone, and L. Verdoliva. Fingerprint liveness detection based on Weber local image descriptor. *Proc. BioMs*, pages 1–5, 2013.

[14] D. Gragnaniello, G. Poggi, C. Sansone, and L. Verdoliva. Wavelet-Markov local descriptor for detecting fake fingerprints. *Electronics Letters*, 50(6):439–441, March 2014.

[15] P. Johnson, R. Lazarick, E. Marasco, E. Newton, A. Ross, and S. Schuckers. Biometric liveness detection: Framework and metrics. *Proc. IBPC*, March 2012.

[16] D. G. Lowe. Distinctive image features from scale-invariant keypoints. *International Journal of Computer Vision*, 60(2):91–110, 2004.

[17] D. Maltoni, D. Maio, A.K. Jain, and S. Prabhakar. *Handbook of Fingerprint Recognition*. Springer, London, U.K., 2009.

[18] E. Marasco, Y. Ding, and A. Ross. Combining match scores with liveness values in a fingerprint verification system. In *Proc. BTAS*, pages 418–425, Arlington, VA, USA, September 2012.

[19] E. Marasco, L. Lugini, B. Cukic, and T. Bourlai. Minimizing the impact of low interoperability between optical fingerprints sensors. In *Proc. BTAS*, pages 1–8, Arlington, VA, USA, September 2013.

[20] E. Marasco and A. Ross. A survey on anti-spoofing schemes for fingerprint recognition systems. *ACM Computing Surveys*, to appear.

[21] E. Marasco and C. Sansone. On the robustness of fingerprint liveness detection algorithms against new materials used for spoofing. In *Proc. Biosignals*, pages 553–558, Rome, Italy, January 2011.

[22] E. Marasco and C. Sansone. Combining perspiration- and morphology-based static features for fingerprint liveness detection. *Pattern Recognition Letters*, 33:1148–1156, 2012.

[23] G.L. Marcialis, A. Lewicke, B. Tan, P. Coli, D. Grimberg, A. Congiu, A. Tidu, F. Roli, and S. Schuckers. First international fingerprint liveness detection competition - LivDet 2009. In *Proc. ICIAP*, pages 12–23, Vietri sul Mare, Italy, September 2009.

[24] Y.S. Moon, J.S. Chen, K.C. Chan, K. So., and K.C. Woo. Wavelet based fingerprint liveness detection. *Electronic Letters*, 41(20):1112–1113, September 2005.

[25] S. Nikam and S. Agarwal. Curvelet-based fingerprint anti-spoofing. *Signal, Image and Video Processing*, 4(1):75–87, January 2009.

[26] K. Nixon, V. Aimale, and R. Rowe. Spoof detection schemes. *Handbook of Biometrics*, 2007.

[27] K. Nixon, R. Rowe, J. Allen, S. Corcoran, L. Fang, D. Gabel, D. Gonzales, R. Harbour, S. Love, and R. McCaskill. Novel spectroscopy-based technology for biometric and liveness verification. *Defense and Security*, pages 287–295, 2004.

[28] S. Schuckers. Spoofing and anti-spoofing measures. *Information Security Technical Report*, 7(4):56–62, 2002.

[29] C. Sousedik and C. Busch. Presentation attack detection methods for fingerprint recognition systems: a survey. *IET Biometrics*, to appear.

[30] B. Tan and S. Schuckers. Liveness detection using an intensity based approach in fingerprint scanner. *Proc. BSYM*, September 2005.

[31] D. Yambay, L. Ghiani, P. Denti, G.L. Marcialis, F. Roli, and S. Schuckers. LivDet 2011 - Fingerprint liveness detection competition 2011. In *Proc. ICB*, pages 208–215, New Delhi, India, March 2012.